Upper-Air Temperature Trends over the Globe, 1958–1989

ABRAHAM H. OORT AND HUANZHU LIU

U.S. Department of Commerce/NOAA, Geophysical Fluid Dynamics Laboratory, Princeton University, Princeton, New Jersey

(Manuscript received 15 August 1991, in final form 22 April 1992)

ABSTRACT

New time series of the hemispheric and global mean temperature anomalies in the troposphere and lower stratosphere are presented for the period May 1958 through December 1989. The statistics are based on objective monthly analyses of all available daily soundings from the global rawinsonde network (~700–800 stations). The results are compared with Angell's earlier statistics based on a subset of 63 stations. Excellent agreement is found with these earlier results as well as with an 11-year set of satellite-derived microwave sounding unit data. These detailed comparisons support the conclusion that the rawinsonde network can provide reliable estimates of the actual interseasonal hemispheric-scale temperature changes that have occurred between the earth's surface and about 20 km (50 mb) height since the 1950s.

1. Introduction

A prominent issue in climate research is whether the present climate is changing or not. In particular, is the troposphere getting warmer, and the stratosphere colder? We address these and related questions in this paper by studying the results of a new global dataset and by making some comparisons with other sets. The primary dataset, the GFDL dataset, is based on all available upper-air stations over the globe for a period of more than 31 years. The basic GFDL record of three-dimensional global monthly temperature fields is more complete and more homogeneous (Oort 1983) than any other upper-air record prepared so far. Our intention here is to discuss a small subset of these data, that is, the hemispheric and global seasonal averages as basic measures of the state of the atmosphere, and to refrain from speculations and "explanations" of what is behind the statistics or what factors may be causing the interannual and interdecadal variations that we observe. The reader is referred to Houghton et al. (1990) for an up-to-date review of possible greenhouse signals.

In order to put the GFDL data in a proper perspective, we present them in the form of extensive comparisons with statistics published earlier in the pioneering studies of Angell and his coworkers (e.g., Angell and Korshover 1983; Angell 1988b, 1990). Angell's studies were done carefully but were based on a very limited portion of the rawinsonde network. Thus, questions have arisen as to the adequacy of the rawinsonde network to represent large-scale spatial averages and the significance or nonsignificance of linear trends in the data.

Besides Angell's studies, almost all temperature records studied so far are for conditions near the earth's surface where the records go back for more than 100 years (see review by Folland et al. 1990). Important recent research on surface temperatures has been reported in, for example, Vinnikov et al. (1990), Hansen and Lebedeff (1988), Jones et al. (1986), and Jones (1988) based on the extensive surface land station network, and in, for example, Folland et al. (1984) and Oort et al. (1987) based on the historical surface ship reports. Recently, microwave data from satellites (Spencer et al. 1990) are raising hopes for a perhaps more representative global monitoring of the earth from space; however, the microwave records are still short and require further research to show what layers in the atmosphere are actually monitored from satellites.

2. Data sources and data reduction

Although the basic daily rawinsonde soundings are from the same global upper-air network, the data archives, data reduction, and analysis schemes used to derive the present statistics (from here on called GFDL data and GFDL statistics) are very different from those used by Angell, as will be discussed.

a. GFDL data

The GFDL data were processed for the 380-month period, May 1958 through December 1989. This was accomplished basically in three separate projects covering the 60-month period May 1958–April 1963 (Oort and Rasmusson 1971), the 120-month period May

Corresponding author address: Dr. Abraham H. Oort, Geophysical Fluid Dynamics Laboratory, U.S. Department of Commerce/NOAA, Princeton University, P.O. Box 308, Princeton, NJ 08542.

1963–April 1973 (Oort 1977, 1983), and the 200-month period May 1973–December 1989. The data sources and data processing schemes were practically identical within each group but there were in general some minor differences between the three groups.

The bulk of the upper-air data for the first period, May 1958–April 1963, came from the Massachusetts Institute of Technology General Circulation Library, which contained daily rawinsonde soundings from about 500 regularly reporting stations taken at 0000 Greenwich mean time over the Northern Hemisphere and was supplemented by daily data from more than 40 tropical stations between latitudes 25°S and 25°N, which were not well represented in the MIT data. After certain crude checks on the basic daily reports were applied monthly mean statistics were computed at each station, which then served as input for the objective analysis scheme (Oort and Rasmusson 1971).

For the second period, May 1963–April 1973, we used the daily soundings routinely received at the National Meteorological Center (NMC) for the purpose of daily weather forecasting as well as a sizeable number of time series of daily soundings from the National Center for Atmospheric Research (NCAR) to fill spatial holes. Initially mainly 0000 UTC (except for the NCAR data), but in the latter half of the period both 0000 and 1200 UTC data were used. The total number of regularly reporting stations had grown to about 700–800. Better checking routines were gradually incorporated for discarding unrepresentative daily reports (Oort 1983).

Finally, for the third period, May 1973–December 1989, we used the twice-daily soundings received at NMC from the greatly improved Global Telecommunication System Network. The global station network was generally as good as or better than the network available during the second period. The checking procedures were very similar to those used during the second period.

To guarantee some degree of stability in the derived monthly statistics we have included only regularly reporting stations. Thus before accepting a station in the global objective analysis scheme for a particular month and at a particular level, we required that the number of acceptable daily reports (N_{days}) for that month and at that level exceeded a specified minimum value. The minimum value was chosen to be $N_{\text{days}} = 10$ (out of a possible 30 or 31) for the first and second periods. In view of the significant improvement in the data during the third period, we increased the cutoff criterion to $N_{\text{days}} = 15$ for the levels below 500 mb but kept $N_{\text{days}} = 10$ at the lower stratospheric levels of 100 and 50 mb with intermediate cutoff values in between. When both 0000 UTC and 1200 UTC data were available the averages for the two times were combined. Therefore, we may expect some weak discontinuities to appear in the time series at those levels where the diurnal variation is important, such as at the lower levels near the earth's surface.

Typical global station distributions at 500 mb are shown in Fig. 1, where the regularly reporting stations are plotted during January of the years 1974 and 1989. The distributions over the continents seem generally adequate during the entire record, except over northeast Africa, South America, and Antarctica. In these last areas, the network is sparse but shows the tendency to improve with time. Over the oceans, especially the Atlantic and Indian oceans, there are some substantial differences in coverage between the three periods. In fact, the gradual demise of the ocean station vessels in the 1980s has made the situation worse over the North Atlantic and northeast Pacific oceans. Overall, however, there has been an increase with time in the number of stations at all latitudes and all levels and a con-

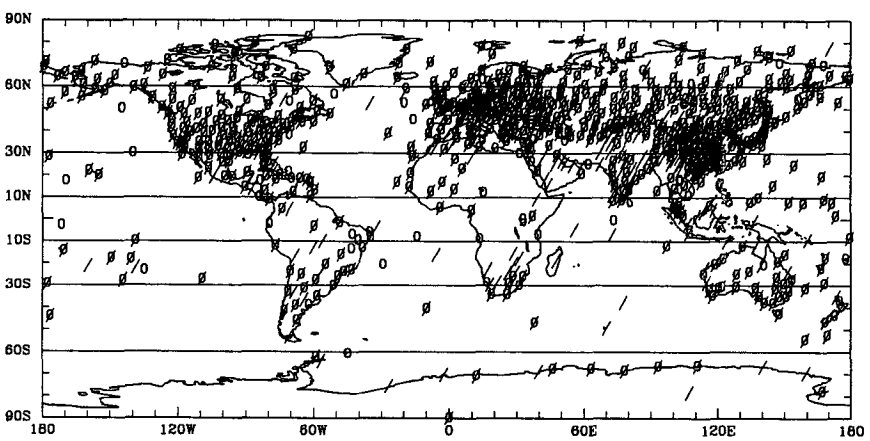

FIG. 1. Global distribution of the regularly reporting (≥10 reports during a month for 0000 or 1200 UTC) rawinsonde stations at 500 mb for the January months of 1974 (774 stations indicated by "0") and 1989 (849 stations indicated by "/"). Most of these stations were used in the objective analyses made at GFDL for each month of the period May 1958 through December 1989 (Oort 1983, updated).

sequent improvement in the global temperature analyses, as shown by the entries in Table 1. The total numbers over the globe during the last 25 years have been on the order of 800 stations or more between 850 and 100 mb. For further information on data coverage, see Oort (1983).

An important data deficiency is evident in the smaller numbers of stations available for the levels below 850 mb, as shown in Table 1. The main reason is that the reports at a standard pressure level are, of course, missing for those days that the surface pressure is less than that standard pressure. Such a lack of data at 1000 mb, and sometimes even at 850 and 700 mb, is most serious in mountainous regions where the station elevations tend to be high. Another factor compounding the problem in the lower layers is that there are no standard reporting levels between 850 and 1000 mb. As a further complication, there can be large diurnal variations in temperature below 850 mb so that once-a-day or even twice-a-day observations are not sufficient to provide representative daily mean values. As we will see later (see Fig. 3), these deficiencies can lead to substantial differences between the time series of mean 1000-mb temperature based on rawinsonde reports and those derived from the more plentiful synoptic surface weather network.

We have used an objective analysis scheme called CRAM (Conditional Relaxation Analysis Method; Harris et al. 1966) to obtain point values at a regular global grid (2.5° latitude, 5° longitude) from the basic station data of the irregular rawinsonde network. The zonal average of the station values in the different latitudinal belts was used as a first guess for the monthly mean temperature fields. In order to minimize the influence of the appearance or disappearance of stations during a particular month, we have analyzed the departures from a 10-year mean climatology for that calendar month. This method leads to much more stable and more reliable results than if the total values were used. The period May 1963–April 1973 was used as the basic climatology. Only during the first five-year period (1958–63) were the total temperature values rather than the anomalies analyzed. This difference in analysis may be responsible for some of the discrepancies between the first 5 years and the later years.

For more detailed information on the analysis methods used, see Oort (1983) and Rosen et al. (1979). The analyses were made for each month of the 380-month period, May 1958 through December 1989, at 11 pressure levels ranging between 1000 mb near the earth's surface to 50 mb in the lower stratosphere. The analyses were for the Northern Hemisphere during the first 60 months, but for the entire globe beginning May 1963.

b. *Angell data*

Angell and his coworkers (e.g., Angell 1988b, 1990) have used a relatively sparse network of 63 carefully

TABLE 1. Number of stations in different climatic zones and at different levels used in the GFDL analyses for the 10-year mean January climatology (1964–1973) (Clim). January 1959, January 1974, and January 1989. The last column contains the number of stations used by Angell.

	1000 mb/sfc				850 mb				500 mb				300 mb				100 mb				50 mb				
	Clim.	1959	1974	1989	Clim.	1959	1974	1989	Clim.	1959	1974	1989	Clim.	1959	1974	1989	Clim.	1959	1974	1989	Clim.	1959	1974	1989	Angell
90°–60°N	90	59	92	83	95	101	107	101	95	102	107	101	94	98	107	101	94	55	107	101	82	25	93	90	8
60°–30°N	235	280	227	251	345	328	407	425	350	342	425	454	349	342	427	451	340	242	417	425	265	136	291	355	12
30°–10°N	74	97	68	88	106	100	117	130	113	106	119	143	110	102	117	134	104	77	109	123	64	41	69	110	12
10°N–10°S	34	18	32	36	39	18	36	39	42	19	38	42	41	17	38	42	38	11	33	39	26	4	26	36	9
10°–30°S	29	18	23	27	43	18	39	52	44	20	40	54	43	20	40	55	40	17	38	52	25	0	23	48	10
30°–60°S	32	—	25	28	46	—	35	39	45	—	35	39	44	—	35	39	42	—	36	37	20	—	20	36	6
60°–90°S	3	—	0	0	15	—	9	14	15	—	9	15	15	—	10	15	13	—	10	16	10	—	9	15	6
Globe	497	472	467	513	689	565	750	800	705	589	774	849	697	579	775	838	672	402	751	794	492	206	532	691	63

selected stations to estimate the temperature variations over the globe. Angell's network is shown in Fig. 2. In the case that a station value was missing during a certain month, a neighboring station, when available, was used instead. Beginning with the year 1958, the International Geophysical Year, through the year 1981, the source of Angell's data has been the mean surface temperature and mean upper-air geopotential height data from the Monthly Climatic Data for the World, published by the National Climatic Data Center (NCDC), NOAA. Beginning in 1980, Angell used data from both the Climatic Data for the World and the Global Telecommunication System Network received at the National Meteorological Center. Comparison of the two datasets helped isolate data problems.

The height data were then used by Angell to compute the thickness of various pressure layers in the atmosphere. The layer thickness basically measures the mean virtual temperature in the layer. Similarly to our approach, Angell used the station anomalies from their long-term climatological mean values (in his case, the 20-year period 1958–77) to arrive at a 33-year time series of seasonal temperature anomalies. There is a slight difference between virtual temperature and temperature itself connected with the presence of water vapor. In general, the differences can be neglected although, in principle, their trends may not be identical since, for example, with global warming also the water vapor content would tend to increase.

Finally, Angell simply averaged the individual station values in seven latitudinal belts, representing the polar (60°–90°), temperate (30°–60°), subtropical (10°–30°), and equatorial zones (10°S–10°N; see last column in Table 1). A 1–2–2–1 weighting (crudely representing the respective areas) of the values in the four zones for each hemisphere then led to the desired hemispheric mean values, and the average of the two hemispheres gave the global mean value.

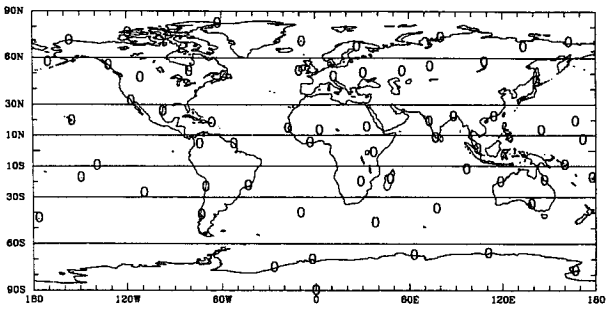

FIG. 2. Global distribution of the 63 rawinsonde stations used by Angell (1988b). Geopotential thickness anomalies for the stations were averaged in belts (e.g., 10°S–10°N, 10°–30°N, 30°–60°N, 60°–90°N), and the resulting values were then averaged (with area weights) to obtain hemispheric and global mean thickness values. The thickness values were used as a measure of the mean layer temperature.

3. Results

The basic GFDL results for the period May 1958 through December 1989 will be presented in terms of seasonal mean time series of temperature anomalies. Plots will be shown for both the Northern and Southern Hemisphere mean values (thick solid curves) at the 950-mb level, and for three layers in the troposphere and lower stratosphere. Because of somewhat better data coverage, the 950-mb statistics (at about 500-m height above sea level) were selected rather than those at 1000 mb for representing the near-surface conditions. In the same figures we will also show Angell's results (thin solid curves) based on his reduced 63-station network. The GFDL–Angell comparisons will enable us to evaluate the relative merits of the two sets of statistics.

a. Surface/950-mb statistics

Over low terrain where the surface pressure is generally on the order of 1000 mb or somewhat larger, the monthly mean temperature anomalies as derived from the daily 950-mb reports at a rawinsonde station should be comparable to the monthly "surface" temperature anomalies measured by a neighboring synoptic weather station at the standard height of about 10 m above the surface; however, strong diurnal variations in the near-surface temperature and missing reports may lead to certain problems, especially in the rawinsonde statistics. Over high terrain, the surface pressure is sometimes less than 950 mb so that the monthly mean 950-mb temperature anomalies may not exist, whereas the surface temperature anomalies should still be available.

In the GFDL 950-mb analyses we have included only those gridpoint values with mean surface pressure greater or equal to 950 mb in order to evaluate the hemispheric and global mean temperature anomalies. On the other hand, Angell used all available surface data from his 63-station network. Thus, the GFDL statistics at 950 mb (see Fig. 3), although they are based on the full rawinsonde network, may be less reliable than the Angell statistics. We have added a constant value of 0.20°C to all GFDL Northern Hemisphere data in Fig. 3 for a better agreement with the Angell and Hansen–Lebedeff curves. The adjustment can perhaps be justified as a tentative gross correction for the predominance of 0000 UTC data in our sample (see later discussion of a possible diurnal bias). Even after this adjustment, the GFDL estimates for the Northern Hemisphere temperature during the 1958–63 period are abnormally low compared to the other curves. Most likely the major cause is again the diurnal bias due to the use of only 0000 UTC data in the early years. In later years progressively more 1200 UTC data were added.

The fairly close similarity shown in Fig. 3 between the results (thin solid lines) for the 63 surface station network and those (dashed lines) of Hansen and Lebedeff (1987, updated) based on all available surface stations (~1500 stations) supports the statement that Angell's 63-station network well represents the inter-

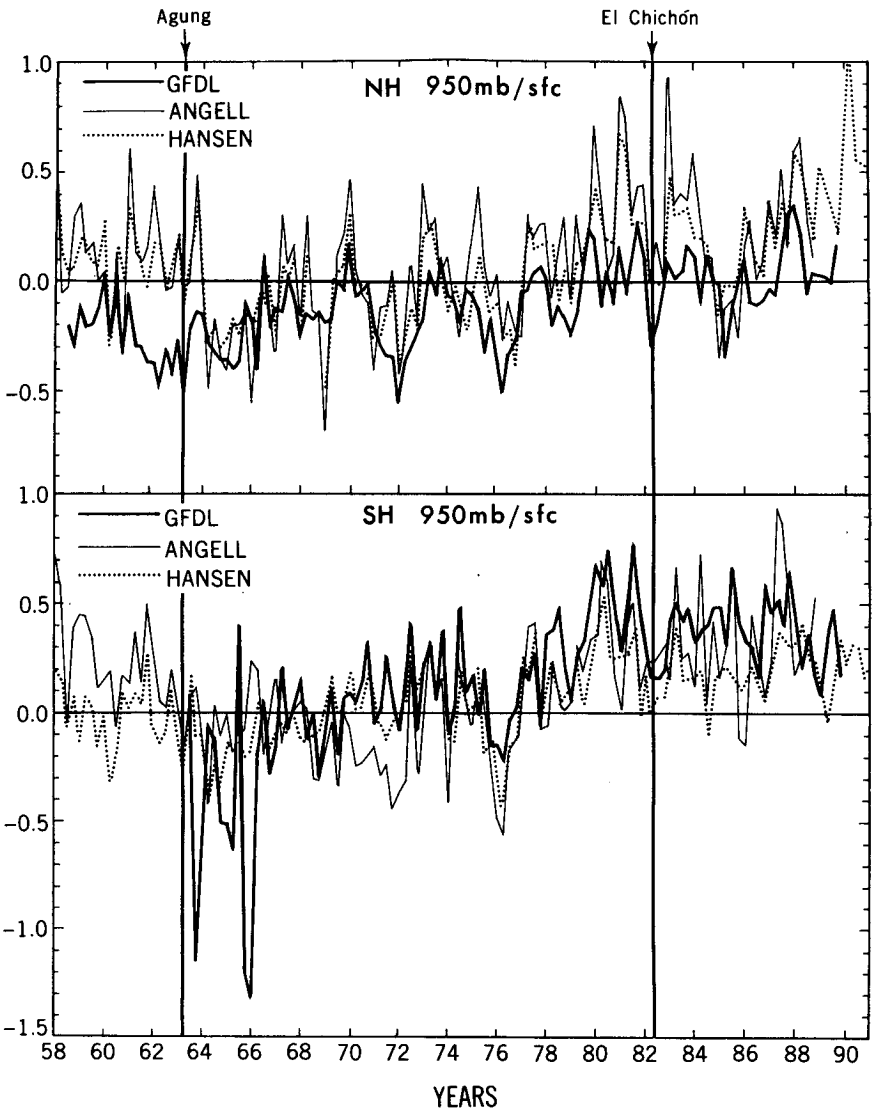

FIG. 3. Time series of the seasonal mean temperature anomalies during the period December 1957–November 1990 for the 950-mb level in the GFDL analyses (thick solid lines) and for the earth's surface in the Hansen and Lebedeff (dashed lines) and Angell (thin solid lines) analyses for the Northern (top) and Southern (bottom) hemispheres. The tick marks along the abscissa at the top and bottom of the figure mark the December–February season of the year shown; for example, the value at 60 indicates the average of the December 1959, January 1960, and February 1960 monthly anomaly values. As expected, due to the smaller number of stations the interseasonal variability is larger in the Angell curves. The correlation coefficients between the GFDL and Angell analyses are $r = 0.39$ for the Northern Hemisphere and $r = 0.41$ for the Southern Hemisphere. The GFDL estimates in the Southern Hemisphere for the SON 1963, SON 1965, and DJF 1966 seasons appear unrealistically low, although no obvious errors were found in the analyses; further, a minor adjustment was made to all GFDL Northern Hemisphere data at 1000 mb by adding a constant value of 0.20°C.

annual hemispheric mean temperature variations near the earth's surface. In fact, the correlation coefficients between the Angell and Hansen–Lebedeff curves shown in Table 2 are high: $r = 0.86$ (0.64) for the Northern (Southern) Hemisphere. It is interesting to note that the correlation coefficients between the Hansen–Lebedeff data and either the Angell or GFDL data are much higher than those between the GFDL and Angell data. In other words, the full surface network used by Hansen–Lebedeff gives the most representative results. Further, as expected from the larger number of stations, the interseasonal standard deviations tend to be smallest for the Hansen–Lebedeff series.

In spite of the low correlation values between the GFDL and Angell time series near the earth's surface, there are some significant similarities when we consider

TABLE 2. Correlation coefficients between the GFDL (950 mb, rawinsonde stations), Angell (63 surface stations), and Hansen–Lebedeff (~1500 surface stations) seasonal temperature anomalies for the JJA 1958 through SON 1989 period for the Northern Hemisphere and for the JJA 1963 through SON 1989 period for the Southern Hemisphere and globe. Also shown are the interseasonal standard deviations in degrees Celsius.

	SH	NH	Globe
GFDL versus Angell	0.41	0.39	0.57
GFDL versus Hansen–Lebedeff	0.66	0.65	0.72
Angell versus Hansen–Lebedeff	0.64	0.86	0.85
σ (GFDL)	0.36	0.18	0.25
σ (Angell)	0.29	0.30	0.25
σ (Hansen–Lebedeff)	0.19	0.22	0.19

the coherence at low frequencies presented in Table 3. The coherence (Panofsky and Brier 1958) can be defined as

$$\mathrm{CH}(i) = \left\{\frac{Q^2(i) + \mathrm{Co}^2(i)}{S_x(i)S_y(i)}\right\}^{1/2},$$

where $Q(i)$, $\mathrm{Co}(i)$, $S_x(i)$, and $S_y(i)$ are the quadrature spectrum, cospectrum, and spectral estimates of the two time series, respectively. We used 28 lags leading to an effective number of Fourier coefficients of 3.5 (Julian 1975), and a 95% significance limit of 0.84. Table 3 shows the results for a few selected representative frequencies (after a 7-point smoother was applied to the individual spectral estimates). We note that at low frequencies the GFDL and Angell time series are coherent for the Northern Hemisphere and the globe but not for the Southern Hemisphere.

During the last 30 years there have been three major volcanic eruptions, those of Mount Agung, Indonesia, in March 1963, El Chichón, Mexico, in April 1982, and Mount Pinatubo, Philippines, in June 1991. According to Angell and Korshover (1983) and Angell (1988a), there is evidence for weak cooling of a few tenths of a degree Celsius in the lower troposphere and much stronger heating in the stratosphere following volcanic eruptions due to the increased dust veil in the lower stratosphere. Angell's (1988a) analyses show that the lowest temperatures near the surface and in the lower troposphere tend to occur on the average about 18 months after a major eruption, and that the highest temperatures in the stratosphere happen much sooner, about 6 to 9 months after a major eruption. The temperature response after the El Chichón eruption does not follow this general pattern, however, due to the simultaneous occurrence of a powerful El Niño that largely offset the volcanic cooling in the lower troposphere. The times of the major eruptions are marked in Fig. 3 as well as in some of the later figures so that the reader may judge to what extent the present data support these claims.

Because the numerical values of the seasonal and annual temperature anomalies for the GFDL analyses may be of wide interest but have not been published before, they are tabulated in Table A1 of the Appendix. In addition, long-term mean values, standard deviations, and least-square trends are presented at the bottom of the table. These quantities are based on the 31-year period, 1959–89, for the Northern Hemisphere and on the 26-year period, 1964–89, for the Southern Hemisphere. The 95% confidence limits for the trends were computed using Spiegel's (1975) formulation, assuming each yearly value to represent an independent estimate. This assumption was tested by Professor Peter Bloomfield from North Carolina State University using a first-order autoregression error model on the data; the results were essentially the same as the present ones. The temperature trends in the GFDL records are of the same order of magnitude (0.1 to 0.3°C/10 yr, depending on the period) as those in the Angell records (see comparisons in Table 4) but they are less reliable for the reasons stated earlier.

We may note that, contrary to expectations, the temperature anomalies tend to be predominantly negative for the 1963–73 period, and that the anomalies do not average out to zero. A likely reason for this discrepancy is that in computing the climatological values the 0000 and 1200 UTC station statistics were given equal weight in spite of the fact that we had 0000 UTC data for all years and 1200 UTC data mainly for

TABLE 3. Estimates of the coherence between the GFDL and Angell seasonal temperature anomaly series for JJA 1963 through SON 1989 for various periods between 14.0 and 0.6 years. Coherence estimates between the GFDL 950-mb and Hansen–Lebedeff surface temperature anomalies are added in parentheses. Significant values (≥0.84, the 95% confidence limit) are printed in italics.

Frequency (yr^{-1})	Period (yr)	950 mb/surface			850–300 mb			300–100 mb			100–50 mb		
		SH	NH	Globe	SH	NH	Globe	SH	NH	Globe	SH	NH	Globe
0.07	14.0	0.76 *(0.91)*	*0.86 (0.92)*	*0.89 (0.93)*	*0.93*	*0.96*	*0.98*	*0.94*	0.68	*0.86*	*0.95*	0.72	*0.91*
0.21	4.7	0.79 *(0.88)*	*0.84 (0.91)*	*0.91 (0.93)*	*0.94*	*0.95*	*0.98*	*0.92*	0.82	*0.88*	*0.93*	0.72	*0.90*
0.50	2.0	0.55 (0.49)	0.61 (0.77)	0.74 (0.74)	*0.86*	*0.94*	*0.94*	*0.85*	*0.94*	*0.90*	0.78	0.72	0.80
0.86	1.2	0.07 (0.26)	0.26 (0.29)	0.06 (0.23)	0.61	0.82	0.77	0.81	*0.86*	0.82	0.40	0.70	0.76
1.65	0.6	0.38 (0.49)	0.20 (0.50)	0.19 (0.36)	0.69	0.67	0.67	0.69	*0.94*	*0.88*	0.68	0.70	0.59

TABLE 4. Comparison between the GFDL and Angell estimates of linear trends (°C/10 yr) in the seasonal temperature anomalies for both a 30-year (December 1958–November 1988) and a 25-year period (December 1963–November 1988). Trend values (±95% significance estimates) are shown for the Northern Hemisphere, Southern Hemisphere, and global mean temperatures, and for the surface–950-mb level and three layers in the troposphere and lower stratosphere. Further, correlation coefficients between the GFDL and Angell time series are presented in the last column using the 1959–88 period for the Northern Hemisphere and the 1964–88 period for the Southern Hemisphere and globe.

	GFDL trend		Angell trend		Correlation coefficient r
	1959–88	1964–88	1959–88	1964–88	
			Surface–950 mb		
NH	0.11 ± 0.04	0.13 ± 0.06	0.09 ± 0.09	0.21 ± 0.10	.39
SH		0.32 ± 0.07	0.08 ± 0.10	0.26 ± 0.08	.41
Globe		0.24 ± 0.06	0.08 ± 0.08	0.23 ± 0.07	.57
			850–300 mb		
NH	0.06 ± 0.09	0.20 ± 0.10	−0.02 ± 0.10	0.12 ± 0.11	.88
SH		0.23 ± 0.09	0.18 ± 0.10	0.33 ± 0.10	.82
Globe		0.22 ± 0.09	0.08 ± 0.10	0.22 ± 0.10	.87
			300–100 mb		
NH	0.03 ± 0.08	−0.03 ± 0.10	−0.20 ± 0.13	−0.11 ± 0.16	.66
SH		−0.11 ± 0.11	−0.16 ± 0.11	−0.25 ± 0.13	.76
Globe		−0.07 ± 0.09	−0.18 ± 0.10	−0.18 ± 0.12	.80
			100–50 mb		
NH	−0.40 ± 0.10	−0.38 ± 0.14	−0.23 ± 0.14	−0.20 ± 0.15	.61
SH		−0.43 ± 0.16	−0.64 ± 0.29	−0.64 ± 0.25	.76
Globe		−0.40 ± 0.12	−0.30 ± 0.16	−0.39 ± 0.17	.66

the later years. Since in the Northern Hemisphere the hemispheric mean temperatures at 950 mb for 1200 UTC tend to be warmer than the corresponding 0000 UTC values by about 0.4°C (see Table 5) due to the position of the major continents in the 0° to 120°E longitude sector, there is a negative diurnal bias in the early individual yearly anomalies (e.g., see Fig. 3, GFDL curve for Northern Hemisphere during 1958–63 period when almost exclusively 0000 UTC data were used in that hemisphere).

b. Statistics of 850–300-mb layer

As a measure of the tropospheric temperature changes, we present the time series of average temperature in the 850–300-mb layer (between about 1.5- and 9-km height) based on the GFDL anomaly analyses at the 850-, 700-, 500-, 400-, and 300-mb levels. The results for the two hemispheres are shown in Fig. 4 together with curves of Angell's results based on his 850–300-mb thickness data. The presentation is similar to the one used for the surface/950-mb time series. We note that the correspondence between the two independent analyses is much better than near the surface with correlation coefficients of $r = 0.88$ and 0.82 for the Northern and Southern hemisphere, respectively, and significant coherences at frequencies of 0.50 yr^{-1} and lower (see Table 3). In the Angell series, the peaks are somewhat higher and the valleys lower than in the GFDL series, as expected from the much smaller number of stations Angell used (63 versus 700 to 800 stations in our case; see Table 1). The GFDL results are also tabulated in Table A2.

If we consider the last 25 years, there is a significant rising trend ranging from 0.1 to 0.3°C/10 yr in the tropospheric temperature, especially in the Southern Hemisphere (see Tables 4 and A2). When we include the earlier five years between 1958 and 1963, only Angell's trend estimate for the Southern Hemisphere is significantly different from zero (at the 95% confidence level). We should note, however, that there was a strong El Niño–Southern Oscillation (ENSO) event around 1957–58. This ENSO event may have been in part responsible for the relatively high temperatures in the beginning of our record and must have contributed to

TABLE 5. Hemispheric and global mean estimates of the annual mean 0000–1200 UTC temperature differences (in °C). The values represent averages over the 21-year period January 1968 through December 1989. In the calculations the monthly temperature anomalies for all "good" ($N_{days} \geq 10$ for each month at each level) rawinsonde stations were averaged in 10° latitude belts for 0000 and 1200 UTC separately. Finally, the zonal mean temperature differences (0000 − 1200 UTC) were calculated and averaged over the hemisphere with the proper area weights.

	1000 mb	950 mb	850–300 mb
NH	−0.74 ± 0.07	−0.39 ± 0.05	−0.13 ± 0.02
SH	−0.18 ± 0.10	−0.07 ± 0.07	−0.11 ± 0.08
Globe	−0.46 ± 0.07	−0.23 ± 0.04	−0.12 ± 0.05

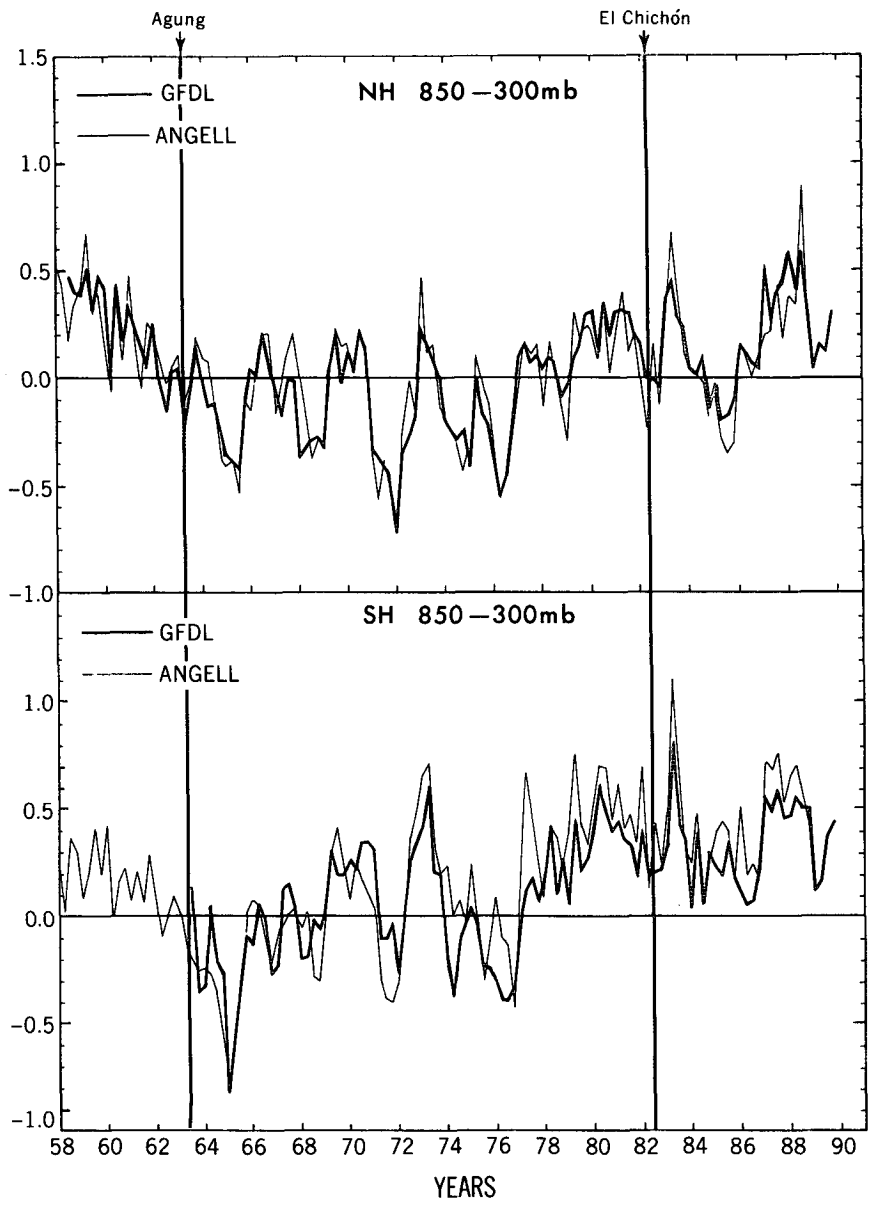

FIG. 4. Time series of the seasonal mean temperature anomalies during the period December 1958–November 1990 for the 850–300-mb layer in the GFDL analyses (thick solid lines) and the Angell (thin solid lines) analyses for the Northern (top) and Southern (bottom) hemispheres. The correlation coefficients between the GFDL and Angell data are $r = 0.88$ (0.82) for the Northern (Southern) Hemisphere.

the relatively low values of the computed 1958–89 temperature trends (e.g., see Angell 1990). As at 950 mb, there is some weak evidence in the 850–300-mb layer for tropospheric cooling after the Mt. Agung and El Chichón volcanic eruptions.

c. Statistics of the 300–100-mb layer

For the upper troposphere (between about 9- and 16-km height) shown in Fig. 5, the agreement between the GFDL and Angell estimates appears still good, with correlation coefficients of $r = 0.66$ and 0.76 for the Northern and Southern hemispheres, respectively. It is interesting to note the unusually high coherence values for this layer at the high frequency end of the spectrum (see Table 3). The strong year-to-year variability in the 300–100-mb layer tends to obscure any possible signal of interdecadal variability in the data. The trend estimates are generally negative, indicating a cooling on the order of -0.1 to -0.2°C/10 yr in the upper troposphere. The Angell and GFDL estimates in the Northern Hemisphere disagree with each other with

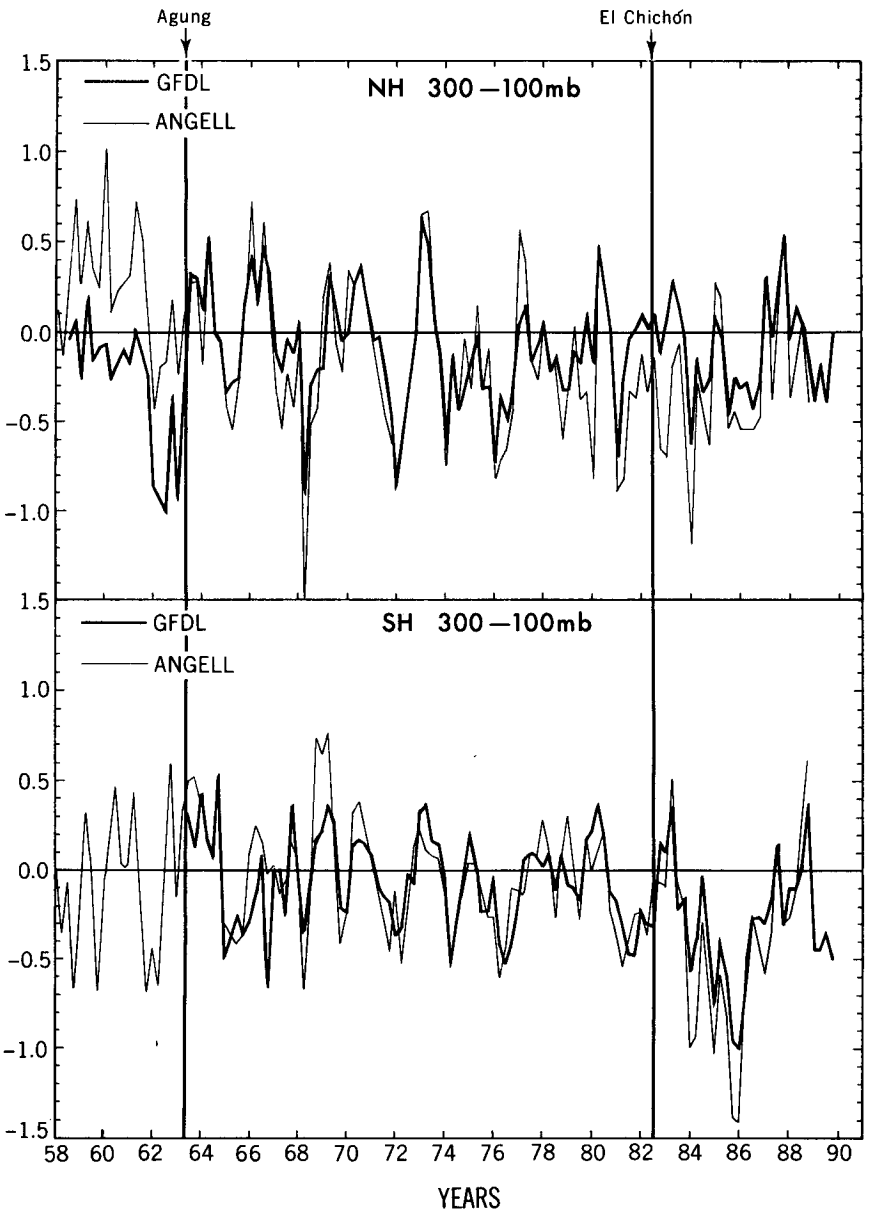

FIG. 5. As in Fig. 4 except for the 300–100-mb layer in the upper troposphere. The correlation coefficients between the GFDL and Angell data are $r = 0.66$ (0.76) for the Northern (Southern) Hemisphere.

significant cooling in the Angell data but no significant cooling trends in the GFDL data (see Tables 4 and A3). The curves in the top portion of Fig. 5 clearly show that the discrepancies are mainly due to differences in the data for the first four years, 1958–62. So far we have not been able to determine the reason for these discrepancies and which data are closer to the true values.

The volcanic effects, if anything, indicate a reversal from the lower tropospheric conditions; that is, a weak heating seems to follow the eruptions. This reversal may be expected with an enhanced absorption of shortwave solar and longwave terrestrial radiation in the dust veil at these heights, and a reduction of solar radiation absorption below the veil (e.g., International Ozone Trends Panel 1988, pp. 490–493).

d. Statistics of the 100–50-mb layer

Finally, we present the results for the highest layer in the GFDL data (between about 16- and 20-km height) in Fig. 6 based on our temperature analyses at 100 and 50 mb. Since the number of station reports decreases noticeably with height especially above 100 mb (see Table 1), both the GFDL and Angell statistics are less reliable than for the lower layers. Nevertheless,

the mutual agreement appears to be almost as good as in the upper troposphere in view of the comparable magnitude of the correlation coefficients and coherence values (see Tables 3 and 4), except in the Northern Hemisphere. The high correlations, however, must be largely due to the similar strong downward trend in temperature in both datasets and not due to similarity in the year-to-year variations that do not track each other very well. The trends are estimated to range from −0.2 to −0.4°C/10 yr in the Northern Hemisphere, and from −0.4 to −0.6°C/10 yr in the Southern Hemisphere (see Tables 4 and A4). This remarkable downward trend was noted before by, for example, Angell (1988b). The (probably too) low estimates of Angell in the Southern Hemisphere for the late 1980s may be connected with a bias in the Angell method of weighting of stations in the Antarctic (60°–90°S) region (Trenberth and Olson 1991; see their Fig. 6). From the GFDL analyses at individual levels (not presented here) we find that the strongest downward trend occurs at the 100-mb level.

The volcanic signal points now to a sizeable heating in the 100–50-mb layer following a major volcanic eruption.

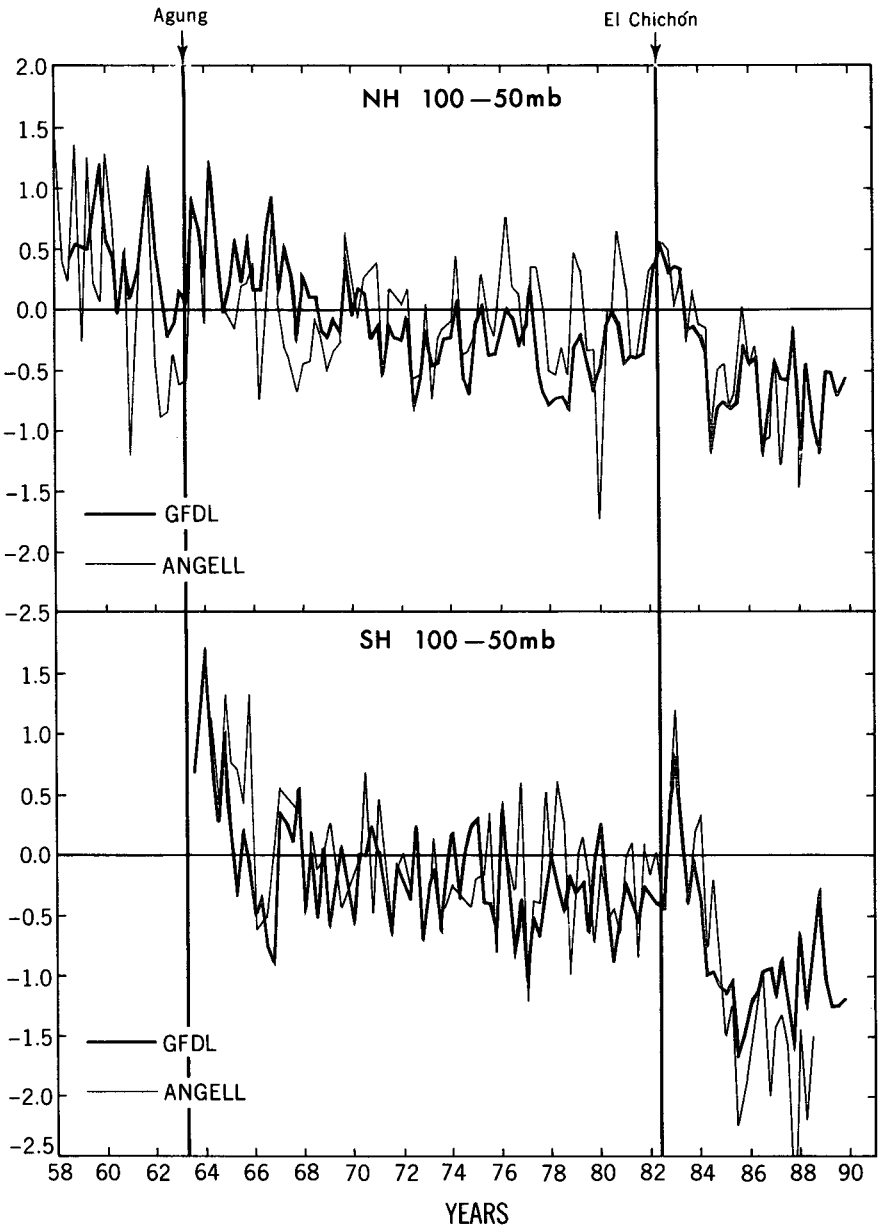

FIG. 6. As in Fig. 4 except for the 100–50-mb layer in the lower stratosphere. The correlation coefficients between the GFDL and Angell data are $r = 0.61$ (0.76) for the Northern (Southern) Hemisphere.

4. Some final comments

So far, we have restricted our discussion to the new GFDL statistics and their comparison with the earlier, more limited, Angell statistics. Here we add some more general comments to put our results in a somewhat broader context.

a. Latitudinal structure of long-term trends

When we consider different latitudinal zones, as shown in Fig. 7, large variations in the temperature trends are found between the different zones. Thus, we find in the troposphere the strongest heating at tropical latitudes and no significant trends at high latitudes. On the other hand, in the lower stratosphere we find excessive cooling at high latitudes around the South Pole and substantial cooling at all other latitudes. The Antarctic cooling suggests a possible connection with the recently discovered depletion of ozone in the Antarctic stratosphere, the so-called ozone hole [see, e.g., observed ozone trends in Stolarski et al. (1991), and general circulation model calculations by Kiehl et al. (1988)]. The depletion became most noticeable in the mid-1980s around the time of the sharp decline in the 100–50-mb temperature shown in Fig. 6.

b. Detection of the greenhouse effect

Model simulations of the expected greenhouse effect due to the historical and future increases in CO_2 and other radiatively active gases generally show tropospheric heating and stratospheric cooling (Manabe and Wetherald 1967, followed by many others; see recent review by Wigley and Barnett 1990). The vertical heating profiles in the models show a rough resemblance to the observed profiles of temperature change as described by Angell (1988) and in the present paper; however, the observed stronger cooling at 200 and 100 mb than at 50 mb (the individual level results are not shown here) is quite different from the model results (with constant ozone amounts) where the strongest cooling is predicted at the highest levels. Nevertheless, the expected sign reversal between the troposphere and stratosphere has been used by, for example, Karoly et al. (1992) in an attempt to get a better handle on the problem of detecting the greenhouse effect. It is likely that the model simulations will become more realistic when also the observed ozone changes will be taken into account (Ramaswamy et al. 1992).

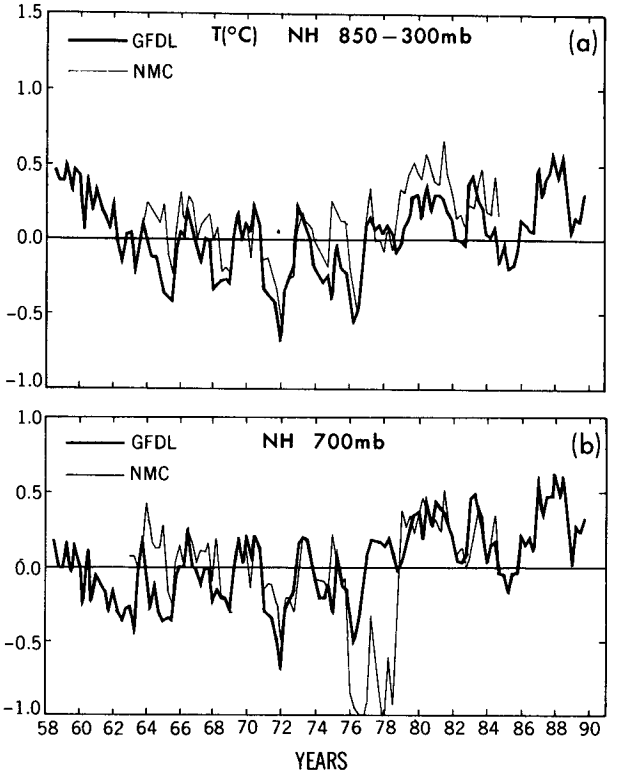

FIG. 8. Intercomparison of two mean temperature analyses based on the GFDL statistically interpolated analyses and the NMC model-interpolated analyses for (a) the 850–300-mb layer and (b) the 700-mb level. Some minor differences may be expected because of the differences in area, that is, the entire NH in the GFDL case and the 20°–90°N area in the NMC case.

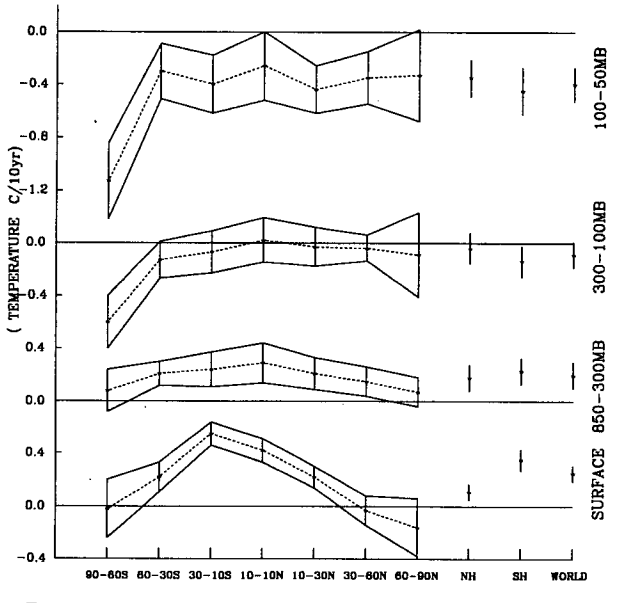

FIG. 7. Latitudinal profiles of the estimated trends in the annual mean GFDL temperatures in °C/10 yr for the 950-mb level and the 850–300-, 300–100-, and 100–50-mb layers during the period December 1963–November 1989. The 95% confidence limits are also shown.

c. The use of model-derived analyses

Model-derived synoptic daily analyses as made, for example, at the National Meteorological Center (NMC) or the European Centre for Medium-Range Weather Forecasts (ECMWF), constitute a different source of climate statistics. These analyses, however, are generally thought to be unusable for climate trend

studies because of the frequent changes in analysis schemes and data input made in attempts to improve the daily weather forecasts. Although the intercomparison for the 850–300-mb layer between GFDL and NMC as shown in Fig. 8a is not too bad, the results for individual levels show some of the inherent problems in using the historical model analyses. For example, in Fig. 8b at 700 mb we find a sudden 1°C drop in the temperature record of the NMC analyses around January 1976 and an equivalent sudden rise around October 1978, both of which must be spurious. Comparisons with the ECMWF analyses show similar problems.

In the near future, however, we can look forward to a new consistent set of historical analyses obtained using a "frozen" general circulation model (GCM). This type of sophisticated interpolation scheme between data points using the basic laws of physics must be, in the long run, superior to our analyses based on a purely statistical interpolation scheme. The so-called "reanalysis" project presently in preparation at NMC for a possible period of 30 years is of great importance; it should eventually be pursued much further back in time before the 1950s (Kalnay and Jenne 1991).

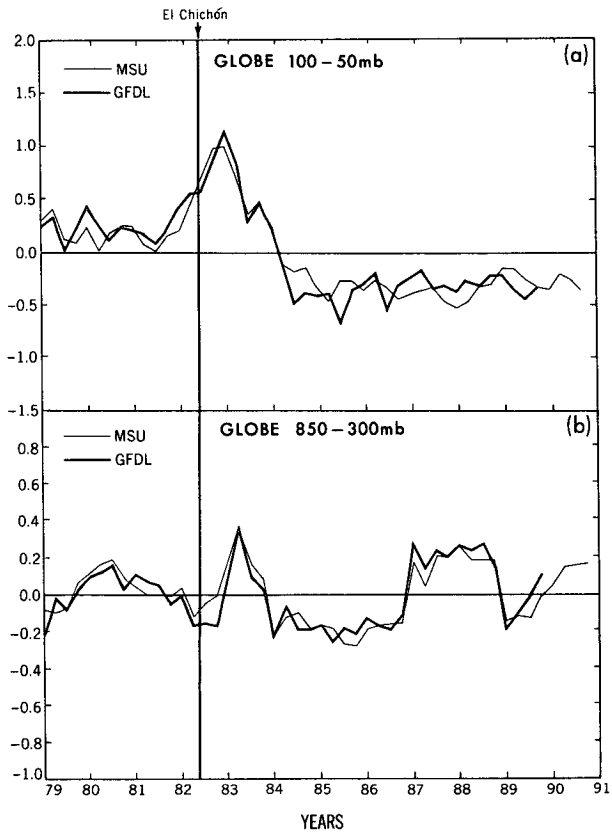

FIG. 9. Intercomparison of the global mean seasonal temperature analyses based on MSU Channels 2 and 4 satellite data (thin solid lines; from Spencer et al. 1990) and on 850–300-mb and 100–50-mb GFDL rawinsonde data (thick solid lines) for the 1979–90 period.

TABLE 6. Comparisons of the GFDL and MSU seasonal temperature series for the 11-year period, DJF 1979 through SON 1989. Presented are correlation coefficients and standard deviations (in °C) for the troposphere and lower stratosphere.

	850–300 mb			100–50 mb		
	SH	NH	Globe	SH	NH	Globe
r (GFDL, MSU)	0.76	0.89	0.91	0.91	0.94	0.94
σ (GFDL)	0.17	0.19	0.17	0.54	0.41	0.41
σ (MSU)	0.16	0.18	0.16	0.45	0.46	0.39

d. Comparison with satellite-derived temperatures

As another completely independent check of the validity and representativeness of our results, we have made a comparison of the GFDL global mean 850–300-mb and 100–50-mb temperature data with the satellite-derived data from channels 2 and 4 of the microwave sounding unit (MSU) presented by Spencer et al. (1990). The satellite data are available since January 1979 so that there is an 11-year overlap with the GFDL analyses. In Fig. 9 the seasonal MSU temperature anomalies are compared with our estimates. In spite of possible biases in both datasets, such as incomplete station coverage in the GFDL data and possible contaminations in the satellite data, the overall agree-

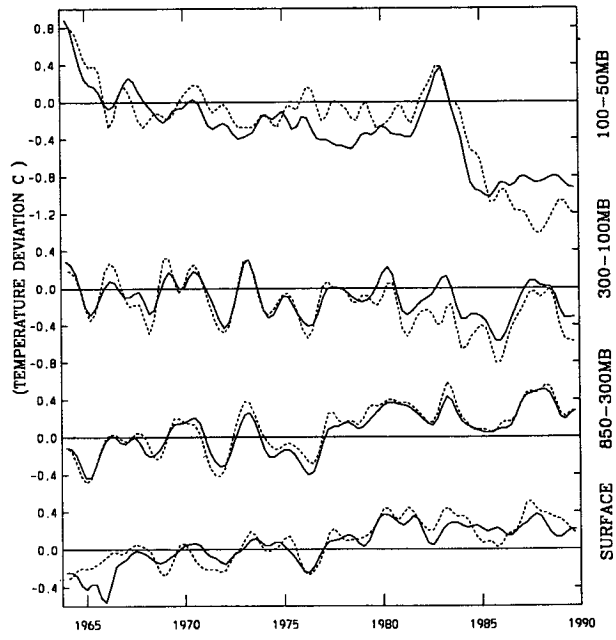

FIG. 10. Smoothed time series of the global mean temperature anomalies in the GFDL (solid) and Angell (dashed) seasonal datasets for the 950 mb-earth's surface, and the 850–300-, 300–100-, and 100–50-mb layers during the 26-year period JJA 1963–SON 1989. The smoothed data were obtained from the seasonal anomalies by applying a three-point smoother ($\frac{1}{4}$–$\frac{1}{2}$–$\frac{1}{4}$) with the exception of the first and last point where a two-point smoother ($\frac{1}{2}$–$\frac{1}{2}$) was used twice. The tick marks along the abscissa mark the northern winter season (December–February) of the year shown.

ment, even in the lower stratosphere, is excellent and adds credibility to both datasets. In fact, the correlation coefficients are on the order of 0.9 both in the troposphere and lower stratosphere, as shown in Table 6. The interseasonal standard deviations are found to be of the same order of magnitude in both datasets.

5. Summary

The GFDL results for the time series between May 1963 and December 1989 are summarized in Fig. 10 after the hemispheric values were combined into global estimates. The successive seasonal values were smoothed first by applying a (1/4–1/2–1/4) weighting filter twice, except at the beginning and end points, where the first two and last two values were averaged. The relatively weak upward trend of temperature in the lower troposphere and the strong downward trend in the lower stratosphere are quite apparent during all seasons. Efforts to model the expected temperature changes due to observed trends in CO_2, O_3, and other trace gases are beginning to throw some light on possible causes of the observed trends reported here.

We conclude, based on the various comparisons shown in this paper, that the rawinsonde network provides adequate information (and has provided that during the last 30 to 40 years) to estimate some of the most important areal-mean climate parameters, such as the hemispheric mean temperature, both for the

TABLE A1. Hemispheric mean temperature anomalies (in °C) at 950 mb for individual seasons and years based on the GFDL analyses for the period May 1958 through December 1989. The anomalies were computed from the 1963–73 mean climatology given in the last line of the table. At the bottom of the table, the values of the long-term mean, standard deviation, and linear trend (in °C/10 yr) based on 31 years for the Northern Hemisphere and 26 years for the Southern Hemisphere are given together with 95% confidence limits for the trend values.

	Northern Hemisphere					Southern Hemisphere				
Year	DJF	MAM	JJA	SON	Year	DJF	MAM	JJA	SON	Year
1958	—	—	−0.21	−0.29	—	—	—	—	—	—
1959	−0.12	−0.21	−0.20	−0.12	−0.16	—	—	—	—	—
1960	0.01	−0.23	−0.03	−0.31	−0.13	—	—	—	—	—
1961	−0.08	−0.31	−0.30	−0.37	−0.30	—	—	—	—	—
1962	−0.38	−0.47	−0.32	−0.42	−0.39	—	—	—	—	—
1963	−0.28	−0.50	−0.23	−0.15	−0.26	—	—	0.08	−1.16	—
1964	−0.15	−0.27	−0.33	−0.36	−0.32	−0.53	−0.07	−0.13	−0.51	−0.31
1965	−0.36	−0.41	−0.37	−0.11	−0.30	−0.51	−0.62	0.41	−1.20	−0.52
1966	−0.19	−0.42	0.08	−0.22	−0.15	−1.30	−0.23	0.03	−0.28	−0.36
1967	−0.13	−0.15	0.01	−0.08	−0.10	−0.17	0.21	−0.08	0.03	0.05
1968	−0.24	−0.15	−0.18	−0.15	−0.20	0.15	−0.11	−0.01	−0.28	−0.11
1969	−0.19	−0.18	0.00	−0.04	−0.06	−0.07	0.07	−0.19	0.07	0.01
1970	0.15	−0.08	−0.04	−0.01	−0.04	0.10	0.05	0.14	0.29	0.12
1971	−0.20	−0.30	−0.35	−0.35	−0.31	−0.05	0.02	0.25	0.05	0.06
1972	−0.55	−0.38	−0.32	−0.25	−0.36	−0.08	0.12	0.42	−0.09	0.13
1973	−0.18	0.04	−0.06	0.08	−0.01	0.21	0.32	0.06	0.38	0.22
1974	−0.07	−0.08	−0.18	−0.04	−0.11	−0.08	0.03	0.49	0.10	0.15
1975	−0.07	−0.14	−0.32	−0.18	−0.18	0.17	0.00	0.18	−0.15	0.02
1976	−0.38	−0.50	−0.34	−0.27	−0.37	−0.14	−0.21	−0.03	0.02	−0.07
1977	−0.06	−0.05	0.03	0.06	0.02	0.20	0.15	0.25	−0.05	0.14
1978	0.01	−0.20	−0.13	−0.17	−0.14	0.37	0.39	0.47	0.21	0.36
1979	−0.26	−0.15	0.01	0.23	−0.01	0.07	0.27	0.32	0.52	0.33
1980	0.18	−0.11	0.03	−0.09	−0.02	0.66	0.58	0.72	0.48	0.59
1981	0.13	−0.05	0.08	0.25	0.14	0.29	0.45	0.77	0.47	0.49
1982	0.08	−0.29	−0.20	−0.04	−0.15	0.29	0.17	0.16	0.20	0.21
1983	0.07	0.01	0.03	0.16	0.09	0.42	0.50	0.42	0.48	0.45
1984	0.12	−0.08	0.10	0.00	0.01	0.32	0.38	0.40	0.49	0.42
1985	−0.01	−0.33	−0.13	−0.03	−0.10	0.49	0.33	0.63	0.42	0.43
1986	0.08	−0.10	−0.13	−0.10	−0.09	0.33	0.30	0.18	0.58	0.37
1987	−0.04	−0.07	0.14	0.29	0.12	0.46	0.52	0.41	0.61	0.50
1988	0.34	0.21	−0.05	0.03	0.12	0.44	0.22	0.36	0.19	0.29
1989	0.02	0.02	−0.02	0.16	0.07	0.09	0.33	0.47	0.18	0.24
Mean	−0.09	−0.19	−0.12	−0.08	−0.12	0.08	0.16	0.27	0.12	0.16
Sigma	0.19	0.17	0.15	0.18	0.15	0.40	0.27	0.25	0.39	0.27
Trend	0.12	0.11	0.08	0.14	0.11	0.38	0.25	0.20	0.37	0.29
	±0.06	±0.05	±0.05	±0.05	±0.04	±0.13	±0.09	±0.09	±0.13	±0.07
Climatology	8.41	12.31	18.30	14.23	13.31	14.68	12.85	9.54	11.14	12.06

Northern and Southern hemispheres. In fact, we have given here, as a function of height, reliable estimates of the seasonal anomalies for individual years as well as representative measures of the interannual variability and the long-term trends for the mean temperature in the troposphere and, to a more limited extent, also in the lower stratosphere.

Acknowledgments. We are grateful to Jim Angell for providing his 63-station statistics; to Peter Bloomfield, Tony Broccoli, and Jerry Mahlman for reviewing the manuscript; to Sara Batata, Mel Rosenstein, and Phil Tunison for preparing the figures; and to Wendy Marshall for typing the manuscript.

APPENDIX

Tables of Hemispheric Mean Temperature Anomalies

Seasonal and annual mean hemispheric temperature anomalies based on the GFDL monthly analyses are tabulated for the 950-mb level in Table A1, and for the layers 850–300 mb in Table A2, 300–100 mb in Table A3, and 100–50 mb in Table A4.

For the Northern Hemisphere, the statistics cover 126 seasons from June–August 1958 through September–November, 1989 and the 31 calendar years 1959 through 1989. In case of the Southern Hemisphere, the seasonal statistics start in June–August 1963 and the annual statistics cover the 26 calendar years, 1964 through 1989. The original monthly anomalies were taken with respect to the May 1963–April 1973 mean climatology for the corresponding calendar month shown in the last line of each table.

At the bottom of each table, long-term mean values (°C), standard deviations (°C), and trend values (°C/10 yr) are given, based on the 31 yearly values in the Northern Hemisphere and 26 yearly values in the Southern Hemisphere. Also, each table shows the 95% significance estimates (Spiegel 1975) for the trend values.

TABLE A2. Same as Table A1 except for the temperature anomalies in the 850–300-mb layer.

	Northern Hemisphere					Southern Hemisphere				
Year	DJF	MAM	JJA	SON	Year	DJF	MAM	JJA	SON	Year
1958	—	—	0.46	0.39	—	—	—	—	—	—
1959	0.38	0.50	0.31	0.47	0.42	—	—	—	—	—
1960	0.41	0.05	0.40	0.18	0.26	—	—	—	—	—
1961	0.32	0.23	0.16	0.06	0.15	—	—	—	—	—
1962	0.23	−0.01	−0.15	0.03	0.03	—	—	—	—	—
1963	0.04	−0.21	−0.06	0.12	−0.01	—	—	0.13	−0.36	—
1964	−0.02	−0.13	−0.12	−0.25	−0.19	−0.32	0.01	−0.22	−0.27	−0.22
1965	−0.36	−0.39	−0.42	−0.12	−0.28	−0.80	−0.56	−0.27	−0.09	−0.40
1966	0.04	0.01	0.20	0.04	0.09	−0.14	0.05	−0.02	−0.28	−0.09
1967	−0.05	−0.17	0.00	−0.01	−0.08	−0.24	0.12	0.15	0.04	0.04
1968	−0.36	−0.31	−0.28	−0.27	−0.32	−0.20	−0.19	−0.02	−0.06	−0.13
1969	−0.31	0.04	0.18	−0.01	0.01	0.04	0.29	0.19	0.19	0.22
1970	0.12	0.04	0.21	0.13	0.07	0.25	0.21	0.34	0.34	0.29
1971	−0.33	−0.37	−0.41	−0.51	−0.42	0.30	−0.11	−0.11	−0.05	−0.02
1972	−0.69	−0.34	−0.27	−0.18	−0.32	−0.24	−0.01	0.25	0.34	0.10
1973	0.21	0.16	0.07	0.00	0.11	0.40	0.58	0.20	0.19	0.31
1974	−0.20	−0.24	−0.29	−0.24	−0.28	−0.20	−0.37	−0.12	−0.04	−0.13
1975	−0.40	−0.03	−0.18	−0.22	−0.19	0.03	−0.06	−0.24	−0.25	−0.18
1976	−0.38	−0.56	−0.46	−0.23	−0.39	−0.30	−0.39	−0.40	−0.34	−0.34
1977	0.10	0.16	0.07	0.10	0.13	−0.03	0.12	0.17	0.06	0.09
1978	0.04	0.11	0.06	−0.08	0.03	0.15	0.44	0.09	0.24	0.22
1979	−0.03	0.09	0.15	0.30	0.15	0.07	0.40	0.21	0.26	0.27
1980	0.31	0.16	0.34	0.20	0.25	0.39	0.60	0.49	0.38	0.47
1981	0.31	0.32	0.30	0.21	0.29	0.43	0.35	0.32	0.20	0.34
1982	0.15	0.00	0.00	−0.04	0.02	0.36	0.18	0.20	0.21	0.21
1983	0.37	0.45	0.28	0.22	0.31	0.32	0.79	0.44	0.36	0.47
1984	0.04	0.02	0.09	−0.15	−0.02	0.03	0.38	0.04	0.28	0.21
1985	−0.04	−0.19	−0.17	−0.10	−0.09	0.22	0.18	0.32	0.18	0.20
1986	0.14	0.12	0.07	0.05	0.11	0.11	0.05	0.07	0.22	0.15
1987	0.50	0.31	0.41	0.47	0.45	0.54	0.48	0.57	0.45	0.52
1988	0.58	0.43	0.56	0.33	0.42	0.46	0.56	0.50	0.50	0.47
1989	0.04	0.16	0.13	0.31	0.18	0.11	0.15	0.36	0.43	0.27
Mean	0.04	0.01	0.04	0.03	0.03	0.07	0.16	0.14	0.13	0.13
Sigma	0.30	0.26	0.26	0.22	0.24	0.31	0.32	0.25	0.24	0.25
Trend	0.06	0.08	0.07	0.05	0.07	0.26	0.22	0.20	0.21	0.22
	±0.10	±0.09	±0.09	±0.08	±0.08	±0.11	±0.13	±0.09	±0.08	±0.09
Climatology	−14.23	−11.51	−6.00	−9.81	−10.39	−9.55	−11.18	−14.10	−12.80	−11.91

TABLE A3. Same as Table A1 except for the temperature anomalies in the 300–100-mb layer.

	Northern Hemisphere					Southern Hemisphere				
Year	DJF	MAM	JJA	SON	Year	DJF	MAM	JJA	SON	Year
1958	—	—	−0.05	0.05	—	—	—	—	—	—
1959	−0.23	0.16	−0.16	−0.09	−0.06	—	—	—	—	—
1960	−0.07	−0.27	−0.19	−0.12	−0.14	—	—	—	—	—
1961	−0.18	0.00	−0.14	−0.25	−0.24	—	—	—	—	—
1962	−0.86	−0.92	−1.00	−0.37	−0.77	—	—	—	—	—
1963	−0.93	−0.42	0.32	0.30	−0.12	—	—	0.31	0.14	—
1964	0.13	0.53	0.01	−0.07	0.12	0.42	0.18	0.08	0.53	0.21
1965	−0.34	−0.28	−0.26	0.18	−0.09	−0.50	−0.40	−0.26	−0.37	−0.35
1966	0.41	0.22	0.46	0.29	0.30	−0.30	−0.16	0.08	−0.67	−0.24
1967	−0.14	−0.23	−0.05	−0.13	−0.13	−0.01	0.00	−0.23	0.36	0.01
1968	0.02	−0.88	−0.28	−0.20	−0.35	−0.03	−0.36	−0.12	0.17	−0.06
1969	−0.21	0.32	0.11	−0.06	0.04	0.22	0.37	0.25	−0.21	0.13
1970	0.00	0.27	0.36	0.16	0.18	−0.23	0.13	0.17	0.15	0.11
1971	−0.05	−0.03	−0.25	−0.45	−0.22	0.08	−0.07	−0.14	−0.17	−0.13
1972	−0.83	−0.52	−0.29	−0.06	−0.36	−0.37	−0.33	−0.03	−0.08	−0.15
1973	0.60	0.49	0.07	−0.13	0.21	0.32	0.37	0.17	0.14	0.23
1974	−0.65	−0.19	−0.44	−0.30	−0.38	−0.05	−0.50	−0.30	−0.05	−0.21
1975	−0.18	−0.03	−0.32	−0.30	−0.24	0.18	0.02	−0.22	−0.23	−0.09
1976	−0.71	−0.37	−0.46	−0.29	−0.42	−0.06	−0.42	−0.53	−0.39	−0.38
1977	0.05	0.15	−0.17	−0.08	0.00	−0.18	0.06	0.09	0.09	0.06
1978	0.05	−0.21	−0.13	−0.32	−0.18	0.02	0.09	−0.10	0.08	0.01
1979	−0.32	−0.12	−0.18	0.07	−0.12	−0.08	−0.09	−0.16	0.16	−0.01
1980	−0.15	0.48	0.21	0.01	0.07	0.23	0.37	0.20	−0.11	0.14
1981	−0.68	−0.26	−0.03	0.01	−0.16	−0.17	−0.30	−0.47	−0.48	−0.35
1982	0.08	0.02	0.10	−0.10	0.03	−0.23	−0.31	−0.32	0.14	−0.18
1983	0.05	0.27	0.14	−0.04	0.08	0.11	0.33	−0.21	−0.16	−0.02
1984	−0.62	−0.19	−0.34	−0.26	−0.32	−0.55	−0.39	−0.06	−0.37	−0.35
1985	0.08	−0.03	−0.47	−0.26	−0.21	−0.75	−0.43	−0.60	−0.95	−0.73
1986	−0.31	−0.29	−0.43	−0.27	−0.30	−0.99	−0.66	−0.27	−0.26	−0.48
1987	0.31	−0.03	0.22	0.54	0.33	−0.30	−0.16	0.14	−0.29	−0.13
1988	−0.02	0.13	0.05	−0.14	−0.10	−0.09	−0.09	0.03	0.36	0.05
1989	−0.37	−0.20	−0.37	0.00	−0.20	−0.45	−0.44	−0.35	−0.50	−0.45
Mean	−0.20	−0.08	−0.12	−0.09	−0.12	−0.15	−0.12	−0.12	−0.12	−0.13
Sigma	0.37	0.34	0.30	0.21	0.23	0.32	0.29	0.23	0.33	0.23
Trend	0.04	0.05	0.00	0.00	0.02	−0.18	−0.11	−0.09	−0.13	−0.12
	±0.13	±0.12	±0.10	±0.08	±0.08	±0.14	±0.13	±0.10	±0.15	±0.10
Climatology	−55.02	−53.54	−51.08	−53.54	−53.29	−52.08	−54.03	−56.55	−55.11	−54.44

REFERENCES

Angell, J. K., 1988a: Impact of El Niño on the delineation of tropospheric cooling due to volcanic eruptions. *J. Geophys. Res.*, **93,** 3697–3704.

——, 1988b: Variations and trends in tropospheric and stratospheric global temperatures, 1958–87. *J. Climate,* **1,** 1296–1313.

——, 1990: Variations in global tropospheric temperature after adjustment for the El Niño influence. *Geophys. Res. Lett.,* **17,** 1093–1096.

——, and J. Korshover, 1983: Global temperature variations in the troposphere and stratosphere, 1958–1982. *Mon. Wea. Rev.,* **111,** 901–921.

Folland, C. K., D. E. Parker, and F. E. Kates, 1984: Worldwide marine temperature fluctuations, 1856–1981. *Nature,* **310,** 670–673.

——, T. R. Karl, and K. Ya. Vinnikov, 1990: Observed climate variations and change. *Climate Change, The IPCC Scientific Assessment,* J. T. Houghton, G. J. Jenkins, and J. J. Ephrams, Eds., Cambridge University Press, 365 pp.

Hansen, J., and S. Lebedeff, 1987: Global trends of measured surface air temperature. *J. Geophys. Res.,* **92,** 13 345–13 372.

——, and ——, 1988: Global surface air temperatures: Update through 1987. *Geophys. Res. Lett.,* **15,** 323–326.

Harris, R. G., A. Thomasell, Jr., and J. G. Welsh, 1966: Studies of techniques for the analysis and prediction of temperature in the ocean, Part III: Automated analysis and prediction. Interim Report, Travelers Research Center, Inc., for U.S. Naval Oceanographic Office, Contract N62306-1675, 97 pp.

Houghton, J. T., G. J. Jenkins, and J. J. Ephraums, Eds., 1990: *Climate Change: The IPCC Scientific Assessment.* Cambridge University Press, 365 pp.

International Ozone Trends Panel, 1988: Report of the International Ozone Trends Panel—1988, World Meteorological Organization, Global Ozone Research and Monitoring Project, Report No. 18, Vol. II., 780 pp.

Jones, P. D., 1988: Hemispheric surface air temperature variations: Recent trends and an update to 1987. *J. Climate,* **1,** 654–660.

——, T. M. L. Wigley, and P. B. Wright, 1986: Global temperature variations between 1861 and 1984. *Nature,* **322,** 430–434.

Julian, P. R., 1975: Comments on the determination of significance levels of the coherence statistic. *J. Atmos. Sci.,* **32,** 836–837.

Kalnay, E., and R. Jenne, 1991: Summary of the NMC/NCAR Reanalysis Workshop of April 1991. *Bull. Amer. Meteor. Soc.,* **72,** 1897–1904.

Karoly, D. J., J. A. Cohen, G. A. Meehl, J. F. B. Mitchell, A. H. Oort, R. J. Stouffer, and R. T. Wetherald, 1992: An example of fingerprint detection of greenhouse climate change. *Clim. Dyn.,* in press.

TABLE A4. Same as Table A1 except for the temperature anomalies in the 100–50-mb layer.

	Northern Hemisphere					Southern Hemisphere				
Year	DJF	MAM	JJA	SON	Year	DJF	MAM	JJA	SON	Year
1958	—	—	0.42	0.54	—	—	—	—	—	—
1959	0.52	0.49	0.80	1.13	0.76	—	—	—	—	—
1960	0.58	0.45	0.00	0.40	0.33	—	—	—	—	—
1961	0.11	0.28	0.72	1.11	0.54	—	—	—	—	—
1962	0.53	0.19	−0.22	−0.12	0.08	—	—	—	—	—
1963	0.14	0.07	0.86	0.68	0.41	—	—	0.68	1.19	—
1964	0.27	1.19	0.57	−0.03	0.52	1.67	0.66	0.27	0.96	0.74
1965	0.17	0.53	0.25	0.55	0.39	0.15	−0.27	0.17	−0.10	−0.01
1966	0.16	0.15	0.63	0.88	0.43	−0.48	−0.35	−0.74	−0.89	−0.56
1967	0.15	0.47	0.30	−0.22	0.20	0.34	0.26	0.12	0.49	0.24
1968	0.26	0.10	0.10	−0.17	0.04	−0.40	0.00	−0.52	0.06	−0.24
1969	−0.23	−0.07	−0.16	0.34	−0.02	−0.55	−0.27	0.04	−0.26	−0.25
1970	−0.04	0.19	0.15	−0.25	0.00	0.49	0.01	0.00	0.23	0.01
1971	−0.13	−0.50	−0.14	−0.23	−0.24	0.02	−0.23	−0.60	−0.11	−0.30
1972	−0.26	−0.08	−0.79	−0.57	−0.47	−0.23	−0.36	0.24	−0.66	−0.21
1973	−0.22	−0.48	−0.43	−0.24	−0.33	−0.33	−0.14	−0.58	−0.12	−0.29
1974	−0.23	0.03	−0.56	−0.68	−0.35	0.15	−0.33	0.04	0.23	0.02
1975	−0.13	0.03	−0.37	−0.37	−0.20	0.34	−0.39	−0.39	−0.58	−0.27
1976	−0.17	0.00	−0.07	−0.28	−0.13	0.36	−0.23	−0.78	−0.38	−0.32
1977	−0.15	0.12	−0.45	−0.67	−0.34	−0.99	−0.52	−0.66	−0.33	−0.55
1978	−0.79	−0.74	−0.71	−0.81	−0.77	−0.02	−0.26	−0.43	−0.17	−0.21
1979	−0.30	−0.19	−0.45	−0.65	−0.37	−0.31	−0.22	−0.59	−0.04	−0.28
1980	−0.48	−0.14	−0.02	−0.14	−0.23	0.25	−0.46	−0.84	−0.50	−0.42
1981	−0.45	−0.38	−0.40	−0.37	−0.36	−0.23	−0.37	−0.54	−0.26	−0.35
1982	0.07	0.40	0.51	0.30	0.36	−0.32	−0.39	−0.43	0.37	−0.14
1983	0.36	0.34	−0.17	−0.14	0.09	0.80	0.28	−0.35	−0.07	0.08
1984	−0.21	−0.35	−1.12	−0.81	−0.66	−0.37	−0.98	−0.96	−1.06	−0.90
1985	−0.76	−0.83	−0.78	−0.31	−0.67	−1.13	−1.04	−1.65	−1.48	−1.35
1986	−0.45	−0.39	−1.19	−0.79	−0.71	−1.25	−1.13	−0.96	−0.94	−1.05
1987	−0.45	−0.57	−0.59	−0.23	−0.47	−1.14	−0.89	−1.18	−1.48	−1.18
1988	−1.17	−0.45	−0.94	−1.16	−0.93	−0.66	−1.18	−0.77	−0.37	−0.74
1989	−0.52	−0.53	−0.71	−0.58	−0.61	−0.99	−1.24	−1.24	−1.18	−1.17
Mean	−0.12	−0.02	−0.17	−0.14	−0.12	−0.22	−0.39	−0.51	−0.33	−0.37
Sigma	0.40	0.43	0.56	0.57	0.44	0.64	0.46	0.48	0.58	0.46
Trend	−0.34	−0.32	−0.46	−0.45	−0.39	−0.43	−0.46	−0.47	−0.46	−0.45
	±0.09	±0.11	±0.13	±0.14	±0.09	±0.26	±0.14	±0.15	±0.22	±0.15
Climatology	−64.98	−62.65	−60.62	−63.42	−62.92	−61.37	−63.85	−65.41	−62.74	−63.34

Kiehl, J. T., B. A. Boville, and B. P. Briegleb, 1988: Response of a general circulation model to a prescribed Antarctic ozone hole. *Nature,* **332,** 501–504.

Manabe, S., and R. T. Wetherald, 1967: Thermal equilibrium of the atmosphere with a given distribution of relative humidity. *J. Atmos. Sci.,* **24,** 241–259.

Oort, A. H., 1977: The Interannual Variability of Atmospheric Circulation Statistics, NOAA Prof. Paper No. 8, U.S. Govt. Printing Office, Washington, D.C., 76 pp.

——, 1983: Global Atmospheric Circulation Statistics, 1958–1973, NOAA Professional Paper No. 14, U.S. Govt. Printing Office, Washington, D.C., 180 pp. + 47 microfiches.

——, and E. M. Rasmusson, 1971: Atmospheric Circulation Statistics, NOAA Professional Paper No. 5, U.S. Govt. Printing Office, Washington, D.C., 323 pp.

——, Y.-H. Pan, R. W. Reynolds, and C. F. Ropelewski, 1987: Historical trends in the surface temperature over the oceans based on the COADS. *Clim. Dyn.,* **2,** 29–38.

Panofsky, H. A., and G. W. Brier, 1958: *Some Applications of Statistics to Meteorology.* The Pennsylvania State University, 224 pp.

Ramaswamy, V., M. D. Schwarzkopf, and K. P. Shine, 1992: Radiative forcing of climate from global stratospheric ozone loss. *Nature,* **355,** 810–812.

Rosen, R. D., D. A. Salstein, and J. P. Peixoto, 1979: Variability in the annual fields of large-scale atmospheric water vapor transport. *Mon. Wea. Rev.,* **107,** 26–37.

Spencer, R. W., J. R. Christy, and N. C. Grody, 1990: Global atmospheric temperature monitoring with satellite microwave measurements: Method and results 1979–84. *J. Climate,* **3,** 1111–1128.

Spiegel, M. R., 1975: *Probability and statistics. Schaum's Outline Series in Mathematics.* McGraw Hill, 372 pp.

Stolarski, R. S., P. Bloomfield, and R. D. McPeters, 1991: Total ozone trends deduced from *Nimbus 7* TOMS data. *Geophys. Res. Lett.,* **18,** 1015–1018.

Trenberth, K. E., and J. G. Olson, 1991: Representativeness of a 63-station network for depicting climate changes. *Greenhouse-Gas-Induced Climatic Change: A Critical Appraisal of Simulations and Observations.* M. E. Schlesinger, Ed., Elsevier, 249–259.

Vinnikov, K. Y., P. Y. Groisman, and K. M. Lugina, 1990: Empirical data on contemporary global climate changes (temperature and precipitation). *J. Climate,* **3,** 662–677.

Wigley, T. M., and T. P. Barnett, 1990: Detection of the greenhouse effect in the observations. *Climate Change, The IPCC Scientific Assessment,* J. T. Houghton, G. J. Jenkins, and J. J. Ephrams, Eds., Cambridge University Press, 365 pp.